



## Chapter V

### A Comparison between Computer Simulations and Approximate Theoretical Results

#### The Density of Particles Released from the Sun

To study the density of particles released from the Sun, we consider the theory of Earl (1976a). He solved the transport equation with the truncated eigenfunction series method. We will compare between the simulations by computer and approximate theoretical results, so we will briefly explain the theory of Earl (1976a) in the following section.

#### Approximate Theoretical Results of Earl

The focused diffusion theory of Earl (1976a) derives the particle distribution function  $f(\mu, z, t)$  using the Fokker-Planck equation

$$\frac{\partial f}{\partial t} + \mu v \frac{\partial f}{\partial z} = \frac{1}{2} \frac{\partial}{\partial \mu} \varphi \frac{\partial f}{\partial \mu} - \frac{V}{2L} (1 - \mu^2) \frac{\partial f}{\partial \mu} \quad (5.1)$$

where  $f$  is the phase space density,  $\mu$  is the cosine of the pitch-angle,  $z$  is the distance along the magnetic field line,  $V$  is the particle speed and  $L$  is the scale length of the magnetic field,  $L \equiv B/(dB/dz)$ . The coefficient of pitch-angle scattering is

$$\varphi(\mu) = A|\mu|^{q-1}(1 - \mu^2), \quad (5.2)$$

where  $q$  is the spectral index for the irregular interplanetary magnetic field, and  $A$  is the amplitude, which according to quasilinear theory depends on the velocity, rigidity and amplitude of field fluctuations (Jokipii 1966).

Earl studied the distribution function by considering scattering, and focusing. He considered the values of  $q$  and  $V/AL$ , where the latter is the ratio of the scattering length  $V/A$  to the focusing length  $L$ . The density of particles after release from the Sun, as approximated by Earl (1976a,b), is of the form  $F_0^+\{z, t\}$ . The function  $F_0^+\{z, t\}$  yields a more accurate particle distribution function when convoluted with a Gaussian:

$$F_0\{z', t'\} = \int_{-\infty}^{\infty} dz_0 \frac{\exp\{-(z - z_0)^2/4D_*t\}}{2(\pi D_*t)^{1/2}} F_0^+\{z_0, t\}, \quad (5.3)$$

where  $D_* = 0.0405(V^2/A)$  is the coefficient of diffusion introduced by Ma Sung and Earl (1978) and Earl (1974a,b),  $t$  is the time of observation, and  $z$  is the distance, with respect to the injection of particles occurred. The definitions of  $z'$  and  $t'$  are  $z' = z + 2(V/A)$  and  $t' = t + (2/V_+)(V/A)$ . These primed variables are with respect to the occurrence of the flare (see Figure 6.1). The value of  $F_0^+\{z_0, t\}$  is

$$F_0^+ = N_0 \exp \left[ - \left( \frac{t}{\sigma_*} \right) - \kappa_2(z + V_c t) \right] \left[ \delta\{z - V_+ t\} + \frac{1}{2V_*} \left[ \frac{1}{\sigma_*} + V_c \kappa_2 + V_+ \left( \kappa_2 - \frac{1}{L} \right) \right] I_0\{y\} + \frac{\kappa_1}{2} \frac{(z + V_- t)^{1/2}}{(V_+ t - z)^{1/2}} I_1\{y\} \right], \quad (5.4)$$

where  $y$ , the argument of the modified Bessel functions is

$$y = \begin{cases} \kappa_1(V_+ t - z)^{1/2}(z + V_- t)^{1/2}, & -V_- t < z < V_+ t \\ 0, & \text{otherwise} \end{cases} \quad (5.5)$$

In equation (5.4) the other parameters are defined by

$$\sigma_* = 2\sigma_1 \quad (5.6)$$

$$V_* = [U_{01}^2 + \frac{1}{4}(U_{00} - U_{01})]^{1/2} \quad (5.7)$$

$$V_c = -\frac{1}{2}(U_{00} + U_{11}) \quad (5.8)$$

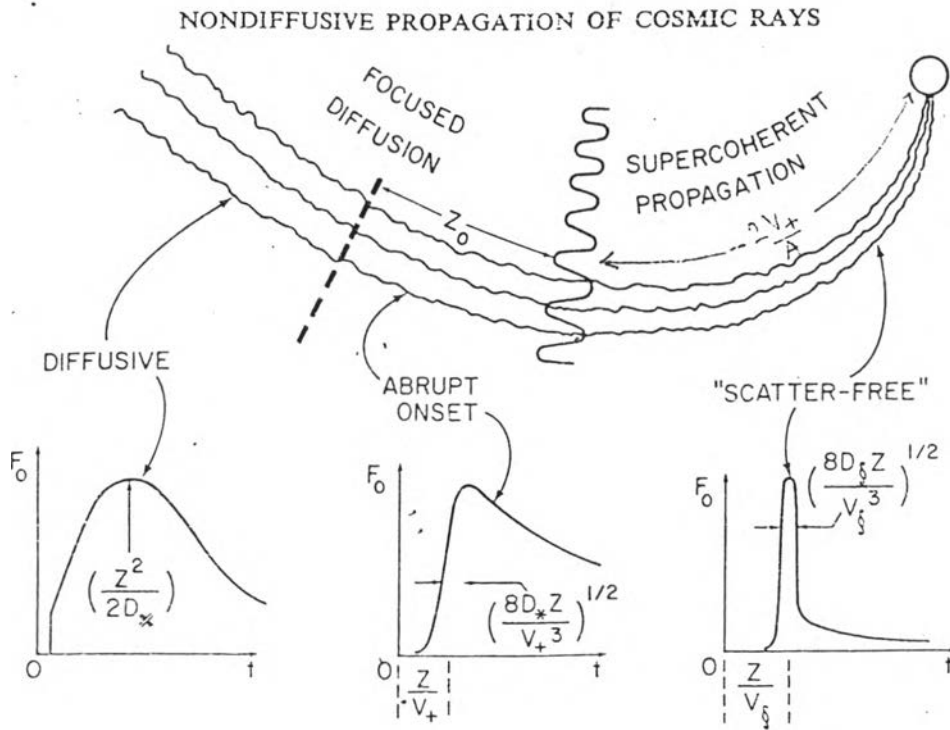


Figure 5.1: Different régimes of solar cosmic ray transport after Earl 1976b.

$$\kappa_1 = \frac{U_{01}}{2\sigma_1 V_*^2} \quad (5.9)$$

$$\kappa_2 = \frac{U_{11} - U_{00}}{4\sigma_1 V_*^2} \quad (5.10)$$

The initial conditions correspond to an injection at  $t = 0, z = 0$  of a pulse moving in the  $+z$  direction with velocity  $V_+$ , so we do not consider  $F_0^-$  when  $V_\dagger = V_+$ . The velocity in the  $+z$  direction is

$$V_+ = V_* - V_c. \quad (5.11)$$

The velocity in the  $-z$  direction is

$$V_- = V_* + V_c. \quad (5.12)$$

Finally, Earl (1976b) describes the particle density in terms of two regions of propagation. The outer region has weak focusing, and a diffusive mode

of propagation is dominant, but coherent modes are stronger as the intensity of focusing increases closer to the Sun. The inner region has strong focusing, and diffusion is weaker, so the propagation is “supercoherent.” Results later in this chapter will show that this separation into regions of “supercoherent” and “coherent” transport is artificial, because the propagation speed steadily decreases with increasing  $z$ .

## The Results of Computational Simulations

We used the wind program for these simulations. Here we used the appropriate versions of files, such as:

f.exp.c for field.c  
 ini\_lowz.c for initial.c  
 inj\_null.c for inject.c  
 p\_zsumf.c for printout.c and  
 s\_abs.c for stream.c

The results for the density of particles injected from the Sun from the wind program and from Earl’s theory appear in the Figures (5.2) and (5.3) respectively. We have normalized Earl’s formula to facilitate the comparison. Note also that Earl’s  $f$  is multiplied by  $e^{z/L}$  to obtain results in terms of our  $F$ . We defined the distance along the field as the abscissa and the pitch-angle averaged density of particles  $\langle F \rangle$  as the ordinate. We found that the basic characteristics of pulses are the same in both figures, so these figures show that we can use the wind program to determine the characteristics of the focused transport of particles from the Sun. In fact, Earl himself uses computer simulations to test the accuracy of his approximate theories (Earl 1994), and the wind program has already been shown to give results similar to those from his program for non-focused transport (Earl et al. 1995).

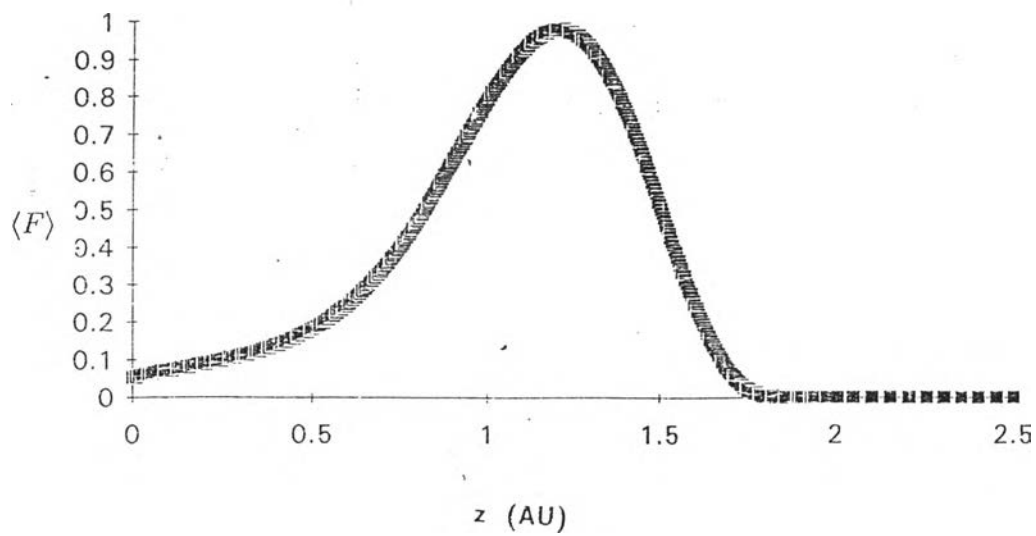


Figure 5.2: Density of particles from wind program simulation.

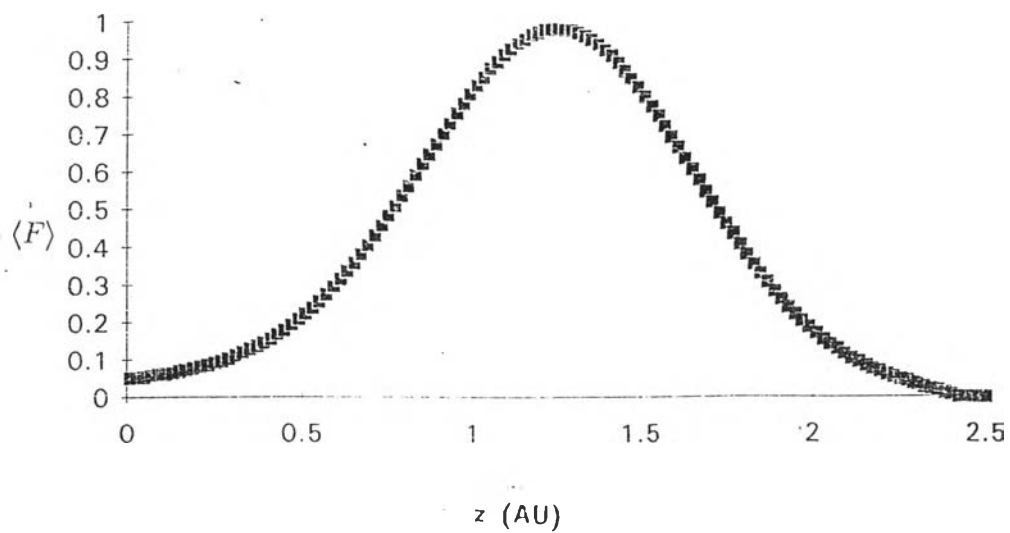


Figure 5.3: Density of particles from Earl's theory.

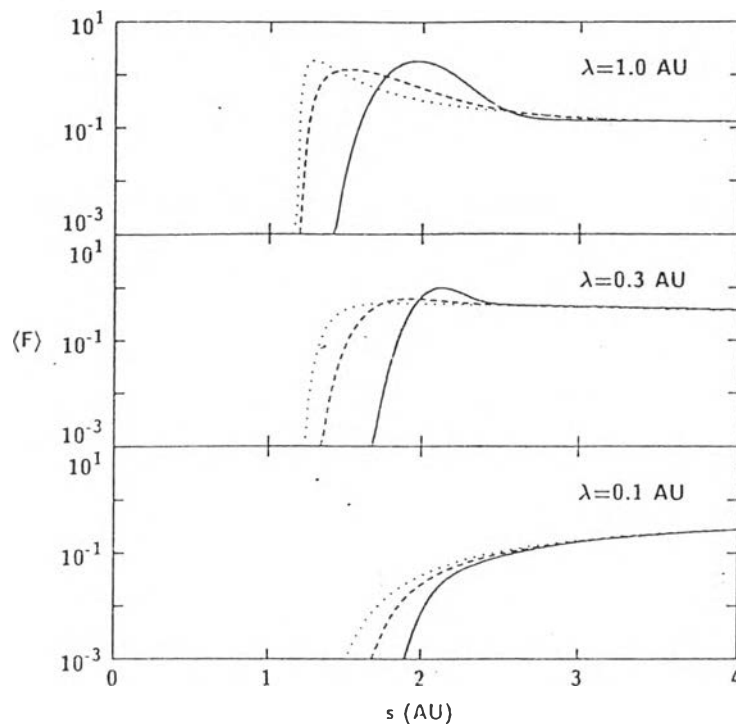


Figure 5.4: Simulation results for  $\langle F \rangle$  at  $r = 1$  AU. versus  $s = vt$  for  $q = 1.0$  (dotted lines),  $q = 1.5$  (dashed lines) and  $q = 1.9$  (solid lines) and for the indicated values of  $\lambda$ .

## Propagation of Coherent Pulses for Various Mean Free Paths $\lambda$ and Indices $q$

Coherent pulses refer to pulses of charged solar cosmic rays of a given energy, which initially tend to travel together with a high anisotropy. From the basis of the transport equation (2.41), we assume that  $v \gg v_{sw}$  and neglect the effects of adiabatic deceleration and convection.

We fit the pitch-angle averaged intensity as a function of  $s = vt$  for the injection of particles near the Sun. We consider various values of  $\lambda$  and  $q$ .

From Figure 5.4, we found that for  $\lambda = 1.0$ , a dominant coherent pulse appears, and the highest peak is for the lowest  $q$ . The profile of a pulse of  $\lambda = 1.0$  is spatially narrow, showing that the concentration of particles is high. For  $\lambda = 0.3$  and lower the height of the peak is smaller than for  $\lambda = 1.0$ . The highest peak is for the highest  $q$ . This Figure (5.4) shows that the late-time

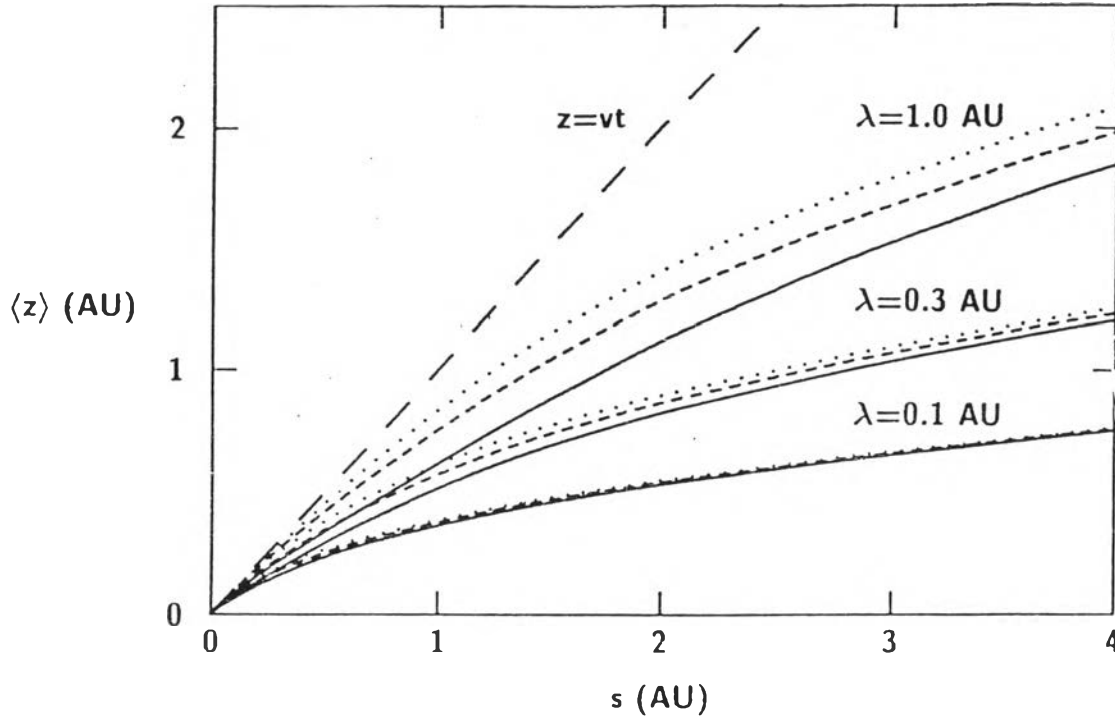


Figure 5.5: Average distance along the magnetic field for various  $\lambda$  and  $q$ .

characteristics for various  $\lambda$  are similar (this is the diffusive region). From the propagation of coherent pulses of particles released from the Sun for various values of the scattering mean free path,  $\lambda$ , and power law index,  $q$ , it is found that the pulse occurs very rapidly. We plot the average distance along the magnetic field of the particle distribution,  $\langle z \rangle$ , for the various values of  $\lambda$  and  $q$  in Figure 5.5. The dashed line,  $\langle z \rangle = s$ , shows the maximum possible distance particles could travel along the magnetic field, with  $\mu = 1$  and  $v_z = v$ .

From Figure 5.5, it is found that the propagation of these particles will follow the magnetic field fastest for the longest mean free path (which implies the weakest scattering). The characteristics of these curves indicate slow motion corresponding to a small mean free path. Note that the rate of change of  $\langle z \rangle$  with respect to  $s$  is

$$\frac{d\langle z \rangle}{ds} = \langle \mu \rangle. \quad (5.13)$$

so  $\langle \mu \rangle$  is proportional to the speed of the pulse. From Figure 5.6 it is found that

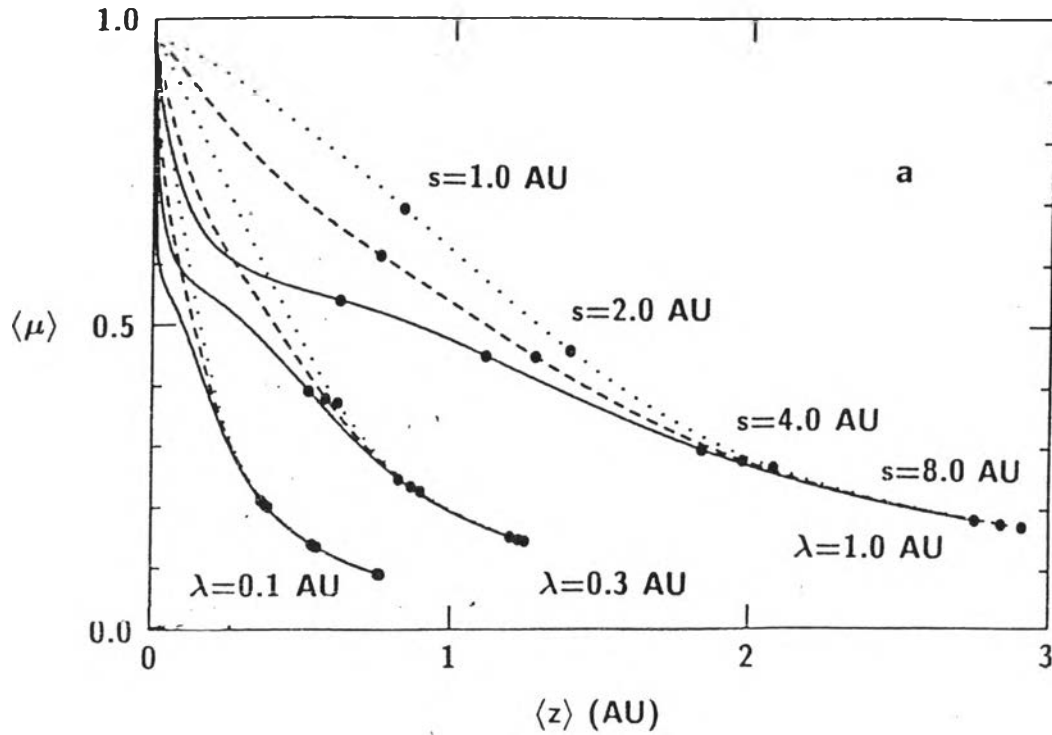


Figure 5.6: Relationship between  $\langle \mu \rangle$  and the average position  $\langle z \rangle$ .

$\langle \mu \rangle$  tends to decrease with the position for every mean free path, and the pulse (as indicated by high  $\langle \mu \rangle$ ) appears in the region that has weak focusing ( $z < \lambda$ ). The convergence of curves for different  $q$  occurs at similar values of  $\langle \mu \rangle \approx 1/3$ . This convergence indicates the decay of the coherent pulse into the diffusive region.

These results from this simulation the propagation of coherent pulses can be compared with theoretical results of Earl (1976a,b) where the focusing length was set to be constant. We find that the speed of propagation is not constant and can not distinguish between supercoherent and coherent regions. Both our work and Earl's indicate that the pulse will occur in the weak focusing region and slowly decay in the diffusive region.